

PCCP

Physical Chemistry Chemical Physics

Accepted Manuscript

This article can be cited before page numbers have been issued, to do this please use: J. Dezalay, E. K. Ashworth, J. E. Fulker, M. H. Stockett, J. A. Noble and J. N. Bull, *Phys. Chem. Chem. Phys.*, 2025, DOI: 10.1039/D5CP02520F.



This is an Accepted Manuscript, which has been through the Royal Society of Chemistry peer review process and has been accepted for publication.

Accepted Manuscripts are published online shortly after acceptance, before technical editing, formatting and proof reading. Using this free service, authors can make their results available to the community, in citable form, before we publish the edited article. We will replace this Accepted Manuscript with the edited and formatted Advance Article as soon as it is available.

You can find more information about Accepted Manuscripts in the [Information for Authors](#).

Please note that technical editing may introduce minor changes to the text and/or graphics, which may alter content. The journal's standard [Terms & Conditions](#) and the [Ethical guidelines](#) still apply. In no event shall the Royal Society of Chemistry be held responsible for any errors or omissions in this Accepted Manuscript or any consequences arising from the use of any information it contains.

Cite this: DOI: 00.0000/xxxxxxxxxx

Cryogenic Action Spectroscopy of the Cyan Fluorescent Protein Chromophore Anion

Jordan Dezalay,^a Eleanor K. Ashworth,^b Jack E. Fulker,^a Mark H. Stockett,^c Jennifer A. Noble,^a and James N. Bull^{*b}

Received Date

Accepted Date

DOI: 00.0000/xxxxxxxxxx

Action spectroscopy at $T \approx 30$ K, as a proxy for the visible absorption band, and the branching between electron detachment and dissociation in the cyan fluorescent protein chromophore anion are reported. The cryogenic action spectra, which show the presence of several rotamers, serve as a reference point for interpreting the effect of nano-environmental interactions in complex protein environments. The adiabatic detachment energy for the lowest energy geometric isomer (Z1) is $19531 \pm 40 \text{ cm}^{-1}$, with the vertical $S_1 \leftarrow S_0$ transition energy at $23734 \pm 40 \text{ cm}^{-1}$. For Z1, the propensity for internal conversion followed by dissociation is low ($<10\%$) compared with autodetachment as the $S_1 \leftarrow S_0$ absorption band is entirely situated in the detachment continuum and is classified as a shape resonance.

Fluorescent proteins (FPs) are the foundation stone of modern, high-resolution bioimaging of cells and the monitoring of microscopic biological processes.¹ Accordingly, a wide range of derivatives of FPs have been developed offering a full colour palette,^{2–5} including cyan fluorescent protein (CFP).⁶ For CFP, mutations over three generations of FPs have substantially improved quantum yield and other fluorescence properties,^{7–9} allowing it to become a widespread biomarker. In several derivative CFPs, including NowGFP and mNeonGreen,^{10,11} the chromophore may be deprotonated and probably resides as the anion (cyan[−]). The optical properties of FPs are dictated by the chromophore unit embedded within a protein binding pocket, with the amalgamation of non-covalent interactions and the local electrostatic field leading to an electrochromic spectral shift and perturbation of the chromophore's intrinsic photophysics.^{12,13} It is of fundamental

importance to characterise the photophysics of FP chromophores in a 'bottom up' approach in order to understand the influence of environment (solvent or protein),¹⁴ and for calibrating or benchmarking of theory.¹⁵

The chromophore in CFP, shown in Fig. 1, is a tryptophan-based derivative of the well known green fluorescent protein (GFP) chromophore. By probing FP chromophores in isolation (i.e. *in vacuo*), their intrinsic photophysics can be elucidated without the complications of solvent effects (e.g. solvatochromic shifts).¹⁶ While the photophysics of the anionic GFP chromophore and substituted forms have been studied thoroughly in the gas phase using action spectroscopy techniques at $T \approx 300$ K,^{17–25} and at

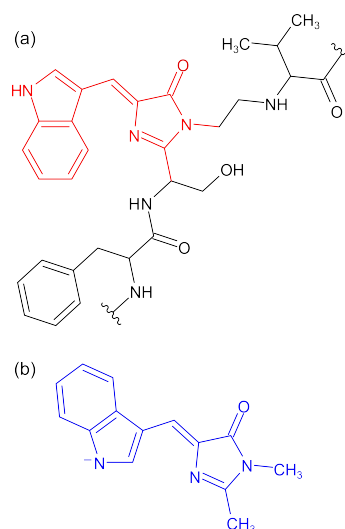


Fig. 1 (a) Structure of the cyan chromophore (red) within CFP, which adopts a Z2 rotamer (i.e. rotation about the central single bond) configuration due to an array of non-covalent interactions. (b) Lowest energy rotamer of isolated cyan[−] (blue), denoted Z1, which has Z-isomer geometry about the methylene bond. For simplicity, we refer to all geometric isomers and rotamers (Z1, Z2, E1, and E2) as isomers. Structures of all isomers are summarised in the ESI.

^a Aix-Marseille University, CNRS, PIIM, Marseille, France

^b Chemistry, Faculty of Science, University of East Anglia, Norwich NR4 7TJ, United Kingdom

^c Department of Physics, Stockholm University, SE-10691 Stockholm, Sweden

* james.bull@uea.ac.uk

† Supplementary Information available: mass spectra demonstrating anion fragments, optimised geometries of possible cyan[−] isomers and rotamers. See DOI: 00.0000/00000000.



cryogenic temperatures,^{26–29} and are largely understood in the gas phase through *ab initio* molecular dynamics simulations,^{15,30} the anionic CFP chromophore is largely unstudied apart from ion storage ring measurements^{31,32} and room-temperature anion photoelectron spectroscopy.³³ It is valuable to perform clear gas-phase experiments on mutant GFP chromophores in order to understand structure-activity trends in the photoactive units of fluorescent proteins.

Here, we characterise the $S_1 \leftarrow S_0$ absorption band and adiabatic electron detachment threshold of isolated cyan[−] at $T \approx 30$ K using action spectroscopy, monitoring photoneutrals (parent and fragment neutrals). Our measurements used the cryogenic ion trap action spectroscopy apparatus at the PIIM laboratory (Aix-Marseille University),^{34,35} where cyan[−] was generated through electrospray ionisation (at $T = 300$ K) of a 1:1 methanol-water solution with a trace amount of ammonia. Significantly, because the chromophore was synthesised stereospecifically as the Z-isomer,²⁵ it is assumed as predominately the Z isomer in the gas phase based on use of ‘gentle’ ion production conditions.²¹ Electrosprayed ions were trapped in a 3D quadrupole ion trap cooled with a helium cryostat; several temperature sensors spread across the ion trap assembly measured temperatures ranging 12–35 K,³⁶ with the contents of the trap expected at $T \approx 30$ K (minimum temperature measured close to the cold head was $T = 21$ K). Since the action spectroscopy is dominated by electron detachment with dissociation being a minor channel, we performed action spectroscopy monitoring parent and fragment neutrals. Here, trapped parent anions were extracted and irradiated (3.62 μ s after extraction) with the laser radiation (EKSPLA NT-342B optical parametric oscillator, ≈ 6 cm^{−1} spectral resolution, calibrated with a wavemeter) in a Gauss tube as part of a time-of-flight region. Parent and fragment anions were decelerated, allowing neutral particles to impact on a microchannel plate detector. Because dissociation is accompanied by kinetic energy release (i.e. fragments moving away from each other), there is a change in the recorded time-of-flight (TOF) profile, allowing the fragment yield to be quantified by analysing laser-on against laser-off TOF profiles. Data were normalised relative to laser-off signal and light fluence. A complete description of the experimental strategies is given in Ref. 37.

To support assignments of the experimental spectra, quantum chemical calculations were performed. Geometries and vibrational frequencies were computed at the ω B97X-D/aug-cc-pVTZ level of theory^{38,39} in Gaussian 16.B01,⁴⁰ while electron detachment energies and vertical excitation energies (VEEs) were computed at the DLPNO-CCSD(T)/aug-cc-pVTZ⁴¹ and STEOM-DLPNO-CCSD/aug-cc-pVTZ⁴² levels of theory using ORCA 6.0.1.⁴³ Absorption profiles ($S_1 \leftarrow S_0$ transition) were simulated using the Franck-Condon-Herzberg-Teller (FCHT) framework as implemented in Gaussian.⁴⁴ The dipole-bound state (DBS) was characterised using the EOM-CCSD/aug-cc-pVDZ+8spd methodology, where +8spd is a series of uncontracted functions (orbital exponents $\zeta = 0.1$ to 2.91×10^{-5} , with geometric progression ratio 3.13)⁴⁵ situated ≈ 5 Å beyond the molecule along the dipole moment vector of the radical neutral (at the anion geometry).

Table 1 Calculated energetics of each cyan[−] isomer (see illustrations in ESI). Relative energy (E_{rel}), vertical excitation energy (VEE) for the $S_1 \leftarrow S_0$ transition, and adiabatic and vertical detachment energies (ADE, VDE) are all given in units of cm^{−1}. Dipole moment magnitudes, $|\mu|$, in Debye.

Species	E_{rel}	VEE	ADE	VDE	$ \mu $
Z1	0	25 121	22 148	23 197	4.75
Z2	66	24 871	22 495	23 455	6.69
E1	720	24 759	22 301	23 197	6.10
E2	2013	24 994	22 648	23 479	6.49

Action spectra recorded over the 19 500–44 000 cm^{−1} (≈ 500 –225 nm) range are shown in Fig. 2a. Parent neutrals were produced in much higher abundance than fragment neutrals across the studied spectral range, demonstrating that autodetachment is much more probable than photoexcitation followed by internal conversion and statistical dissociation. The spectra reveal three bands, labelled A, B, and C, which are present in both parent neutral and fragment neutrals spectra. These are assigned as A – E1 & E2 isomers, B – Z2 isomer, and C – Z1 isomer. This assignment is consistent with the bands intensities and expected gas-phase populations ($T = 300$ K Boltzmann followed by rapid cooling and kinetic trapping). Specifically, from the relative energies in Table 1, a ratio of 100:73 for Z1:Z2 is predicted, which is in good agreement with the experimental band intensities. A small amount of E1 and E2 may be produced through collisions in low vacuum regions (the nascent population of E1 at $T = 300$ K is $\approx 3\%$).²¹ Additionally, the ordering of computed VEEs (Table 1) is consistent with the band assignments. For each of the four isomers, the $S_1 \leftarrow S_0$ transition is bright (oscillator strengths $f = 0.6$ for Z1), while the VEE for the $S_2 \leftarrow S_0$ transition is calculated at 27 000–30 000 cm^{−1} but with $f \approx 10^{-2}$.

A higher resolution spectrum for the parent neutral over the $S_1 \leftarrow S_0$ transition is shown in Fig. 2b. There is no obvious vibrational structure, which parallels observations for action spectra of protonated cations of cyan similarly recorded at $T \approx 20$ K. FCHT simulations predict the transitions for the Z1 and Z2 isomers to be origin dominated, although the overlap of spectra due to multiple isomers complicates an experiment-theory comparison. Our FCHT simulations, included in Fig. 2b, indicate the spectrum should be dominated by contributions from a ≈ 70 cm^{−1} mode (torsion of the single bond on the methylene bridge), and with higher frequency combination bands and indole ring modes result in a congested spectral profile. An earlier room-temperature photoneutrals spectrum of cyan[−] revealed a single peak with wavelength of maximum response at ≈ 459 nm ($\approx 21\,790$ cm^{−1}),³¹ which is red shifted by ≈ 2000 cm^{−1} compared with the most intense band (C) present in the cryogenic spectrum ($23\,835 \pm 50$ cm^{−1}, Fig. 2). STEOM-DLPNO-CCSD calculations on excited states of the radical neutrals produced energies outside of our spectral window, consistent with no direct detachment channels that could account for bands A, B, or C. This result is consistent with expected radical neutral excited states for the related green fluorescent protein chromophore anion.²⁰



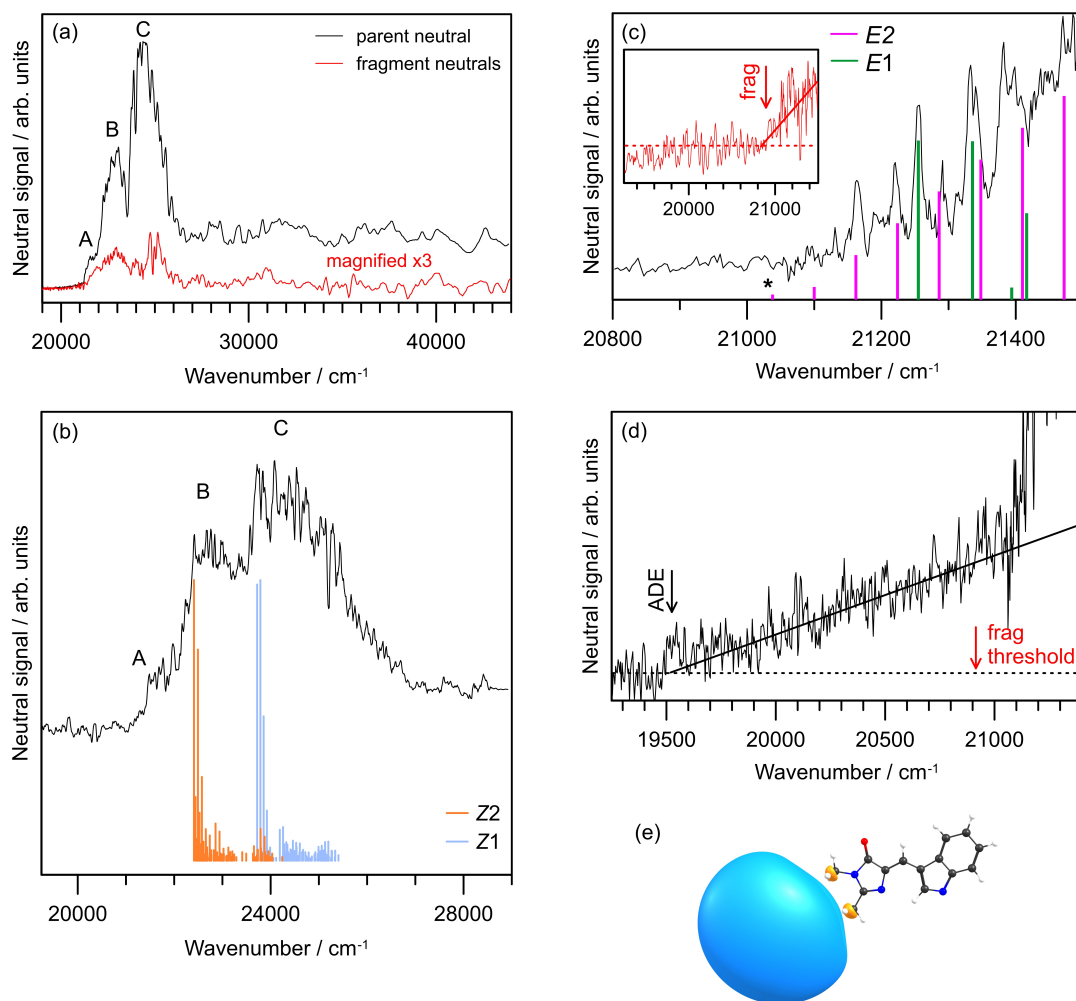


Fig. 2 Action spectra of cyan^- recorded at $T \approx 30$ K: (a) Complete spectra recorded for parent neutral signal (black) and fragment neutrals, 0.5 nm step size. (b) Higher resolution scan (black) over the main group of transitions, 0.2 nm step size. Franck-Condon-Herzberg-Teller ($S_1 \leftarrow S_0$) simulations for the Z1 (blue) and Z2 (orange) isomers are shown and were translated so that respective 0-0 transitions match the onset of the two spectral bands. (c) Higher resolution scan (0.06 nm step size) over region A, assigned to weak signal from E1 (green) and E2 (magenta) isomers. The red inset corresponds to fragment neutrals, with a threshold extrapolated at $\approx 20900 \text{ cm}^{-1}$. The * denotes simulated hot-band signal from E1, which correlates with the fragment neutrals threshold (see inset). (d) Extrapolation of parent neutral signal to the adiabatic detachment energy (ADE) threshold at $19531 \pm 40 \text{ cm}^{-1}$. No fragment neutrals signal was detected for $h\nu < 20900 \text{ cm}^{-1}$ (see inset in c). (e) Calculated DBS orbital for the Z1 isomer with isosurface value 0.005 au, with binding energy 41 meV ($\approx 330 \text{ cm}^{-1}$).

The parent neutral spectrum recorded over band A is shown in Fig. 2c, revealing clear vibrational structure starting at $\approx 21100 \text{ cm}^{-1}$. The spectral position of this vibrational structure was not consistent with any hot band simulations for the Z1 or Z2 isomers; hot band signal extending from band C or B over band A would require ions with room-temperature or warmer internal energies. However, FCHT simulation shows that band A is consistent with small quantities of the E1 and E2 isomers (expected at $\approx 3\%$ from an initial Boltzmann thermal population). The FCHT simulation shows that the E1 isomer is dominated by the origin and first excited vibration of the $\approx 62 \text{ cm}^{-1}$ torsion mode, although the E2 isomer shows an extended progression dominated by a 62 cm^{-1} mode and is because of the steric hindrance and consequential non-planarity of the E2 isomer (leading to the highest E_{rel} value in Table 1), i.e. the excited state for E2 is non-planar. The inset in Fig. 2c shows that weak signal as-

sociated with fragment neutrals is observed from $\approx 20900 \text{ cm}^{-1}$, consistent with assignment of band A to electronically excited anionic states rather than linked with a direct photodetachment processes. Assignments of the labelled vibrations in Fig. 2c are given in the ESI.

While the fragment neutral signal threshold is $\approx 20900 \text{ cm}^{-1}$ (Fig. 2c, inset), the parent neutral threshold was extrapolated to lower wavenumber of $19531 \pm 40 \text{ cm}^{-1}$ (Fig. 2d), which defines the adiabatic detachment energy (ADE). We assign this value to the Z1 isomer since it is the most abundant gas phase species and because calculated ADEs for each isomer (Table 1) indicates that Z1 occurs at the lowest energy. The calculated value (Table 1) is $\approx 2600 \text{ cm}^{-1}$ higher in energy. Since the direct photodetachment signal is so weak compared with autodetachment from the overlapping $S_1 \leftarrow S_0$ transition, it is not possible to discern a reliable VDE value. Room-temperature



photoelectron spectroscopy measurements on cyan[−] have stated VDE = 2.75 ± 0.02 eV (22 177 ± 161 cm^{−1}),³³ which is likely complicated by large autodetachment signals considering the photon energies chosen in that study. It is also worth noting that our fragment neutral signal threshold at ≈20 900 cm^{−1} is consistent with the critical energy threshold (kinetic shifted dissociation threshold) from a recent cryogenic ion storage ring study.³²

TOF mass spectrometry confirmed that the neutral fragments, which are produced in low quantity (<10%) compared with parent neutral signal, are linked with production of anions with *m/z* 223 (−CH₃) and *m/z* 153 (likely involves intramolecular rearrangement), with the former being the predominant photofragmentation pathway for the GFP chromophore anions.^{24,46} The bond dissociation energy (BDE) for the −CH₃ channel is ≈1.6 eV (≈12 900 cm^{−1}),³¹ which is ≈6600 cm^{−1} below the adiabatic detachment threshold. We consequently expect that the small amount of S₁ population following photoexcitation that is able to internally convert to recover the ground electronic will undergo dissociation rather than thermionic emission. In turn, this implies that the parent neutral spectrum should be predominately from direct photodetachment and autodetachment processes.

It is worth noting that the parent neutral cores for each isomer of cyan have permanent dipole moments that support a (non-valence) DBS since $|\mu| > 2.5$ D (Table 1).^{47,48} The calculated DBS orbital for the Z1 isomer is shown in Fig. 2e with calculated binding energy of 41 meV (≈330 cm^{−1}). As expected, the orbital is localised in the direction of the positive end of the molecular dipole moment for the neutral core. Because the oscillator strength to excite the DBS is $f < 10^{-4}$, such states are only observed clearly, e.g. the ground vibrational state through two-photon detachment⁴⁹ or collisional detachment,^{50,51} when the spectroscopic focus is not on nearby valence-localised states with oscillator strengths four to five orders of magnitude higher (Z1, $f \approx 0.6$ for the S₁ ← S₀ transition).^{52,53} Furthermore, cryogenic action spectroscopy on deprotonated indole similarly saw no clear individual DBS transitions in the vicinity of the detachment threshold (rather a broad, unresolved distribution),⁵⁴ while other nitrogen-conditioning PAHs show clearly resolved DBS vibrations. We conclude that DBS transitions are very weak in cyan[−] action spectra, and are swamped by the other excitation processes and are consequently not important in the action spectroscopy of cyan[−].

In some ways, the cryogenic action spectra for cyan[−] contrast with those recorded for the GFP chromophore anion. The latter may exist as *E* and *Z* geometric isomers in the gas phase,²¹ but is not complicated by rotamers due to the symmetry of a *para*-phenoxide moiety rather than the deprotonated indole group in cyan[−]. Moreover, the GFP case shows clear vibrational structure with a pronounced ≈80 cm^{−1} progression assigned to the methine bridge bending/ring scissoring mode from FCHT simulations.^{27,28} Significantly, in the case of the GFP chromophore anion, the S₁ ← S₀ absorption band extends over the detachment threshold with experiments showing differing electron detachment to dissociation branching occurring when tuning laser wavenumber over the band due to a small excited state barrier (≈250 cm^{−1}) to an internal conversion coordinate.^{26,28} This interpretation has been further evidenced by recent cryogenic gas-

phase fluorescence measurements.²⁹ Contrastingly, for cyan[−], the electron detachment threshold (for Z1) is situated 1500–2000 cm^{−1} below the onset of the S₂ ← S₁ transition. Thus, the S₁ excited state in cyan, which is classified as a shape resonance, is entirely situated above the detachment threshold. In such a case, we expect the shape resonance lifetimes to be on the order of tens to hundreds of femtoseconds and, consequently, to show lifetime broadening.^{16,55} On the other hand, the weak photodetachment signal associated with the *E1* and *E2* isomers (which is red-shifted compared with the *Z*-isomers and the *E*-isomers have higher calculated ADE values, Table 1) shows progressions with simulated 62 cm^{−1} spacing, consistent with twisting of the methine bridge and resolved vibrational structure due to a longer excited-state lifetime.

In summary, cryogenic action spectroscopy of cyan[−] has characterised the S₁ ← S₀ absorption properties for the Z1, Z2, *E1* and *E2* isomers, and the adiabatic electron detachment thresholds for the Z1 isomer. The lack of clear vibrational structure, for the major isomer, Z1, is attributed to some combination of congested vibronic transitions and lifetime broadening effects due to prompt autodetachment. The presence of two rotamers for the gas-phase anion is expected to translate to solution, although the abundance of each rotamer will depend on specific solvent-molecule interactions. Consequently, studies of the chromophore in solution, e.g. using ultrafast spectroscopy, that pump on the red vs blue edge of the absorption band will probe differing conformer distributions.

Acknowledgements

This work was funded by an EPSRC New Investigator Award (EP/W018691 to JNB) and the Swedish Foundation for International Cooperation in Research and Higher Education (STINT) Grant for Internationalisation programme (PT2017-7328 to MHS and JNB). EKA thanks the University of East Anglia for a doctoral studentship.

Conflicts of interest

There are no conflicts to declare.

Data availability

The data that support the findings of this study are available from the corresponding author upon reasonable request.

Notes and references

- 1 *Fundamentals of Fluorescence Imaging*, ed. G. Cox, Jenny Stanford Publishing, 2019.
- 2 G.-J. Kremers, J. Goedhart, E. B. van Munster and T. W. J. Gadella, *Biochemistry*, 2006, **45**, 6570–6580.
- 3 G. D. Malo, L. J. Pouwels, M. Wang, A. Weichsel, W. R. Montfort, M. A. Rizzo, D. W. Piston and R. M. Wachter, *Biochemistry*, 2007, **46**, 9865–9873.
- 4 B. Seefeldt, R. Kasper, T. Seidel, P. Tinnefeld, K.-J. Dietz, M. Heilemann and M. Sauer, *J. Biophotonics*, 2008, **1**, 74–82.
- 5 J. S. Paige, K. Y. Wu and S. R. Jaffrey, *Science*, 2011, **333**, 642–646.



- 6 R. Heim, D. C. Prasher and R. Y. Tsien, *Proc. Natl. Acad. Sci.*, 1994, **91**, 12501–12504.
- 7 G. Gotthard, D. von Stetten, D. Clavel, M. Noirclerc-Savoye and A. Royant, *Biochem.*, 2017, **56**, 6418–6422.
- 8 M. L. Markwardt, G.-J. Kremers, C. A. Kraft, K. Ray, P. J. C. Cranfill, K. A. Wilson, R. N. Day, R. M. Wachter, M. W. Davidson and M. A. Rizzo, *PLoS ONE*, 2011, **6**, e17896.
- 9 J. Goedhart, D. von Stetten, M. Noirclerc-Savoye, M. Leimousin, L. Joosen, M. A. Hink, L. van Weeren, T. W. J. Gadella and A. Royant, *Nat. Comm.*, 2012, **3**, 751.
- 10 K. Sarkisyan, A. Goryashchenko, P. Lidsky, D. Gorbachev, N. Bozhanova, A. Gorokhovatsky, A. Pereverzeva, A. Ryumina, V. Zherdeva, A. Savitsky, K. Solntsev, A. Bommarius, G. Sharonov, J. Lindquist, M. Drobizhev, T. Hughes, A. Rebane, K. Lukyanov and A. Mishin, *Biophys. J.*, 2015, **109**, 380–389.
- 11 L. Zarowny, D. Clavel, R. Johannson, K. Duarte, H. Depernet, J. Dupuy, H. Baker, A. Brown, A. Royant and R. E. Campbell, *Protein Eng. Des. Sel.*, 2022, **35**, gzac004.
- 12 M. A. Steffen, K. Lao and S. G. Boxer, *Science*, 1994, **264**, 810–816.
- 13 M. Saggiu, S. D. Fried and S. G. Boxer, *J. Phys. Chem. B*, 2019, **123**, 1527–1536.
- 14 A. Fatima, E. K. Ashworth, I. Chambrier, A. N. Cammidge, G. Bressan, S. R. Meech and J. N. Bull, *Phys. Chem. Chem. Phys.*, 2025, **27**, 9407–9416.
- 15 N. H. List, C. M. Jones and T. J. Martínez, *Chem. Sci.*, 2022, **13**, 373–385.
- 16 E. K. Ashworth, M.-H. Kao, C. S. Anstöter, G. Riesco-Llach, L. Blancafort, K. M. Solntsev, S. R. Meech, J. R. R. Verlet and J. N. Bull, *Phys. Chem. Chem. Phys.*, 2023, **25**, 23626–23636.
- 17 L. H. Andersen, H. Bluhme, S. Boyé, T. J. D. Jørgensen, H. Krogh, I. B. Nielsen, S. Brøndsted Nielsen and A. Svendsen, *Phys. Chem. Chem. Phys.*, 2004, **6**, 2617–2627.
- 18 M. W. Forbes and R. A. Jockusch, *J. Am. Chem. Soc.*, 2009, **131**, 17038–17039.
- 19 C. R. S. Mooney, M. E. Sanz, A. R. McKay, R. J. Fitzmaurice, A. E. Aliev, S. Caddick and H. H. Fielding, *J. Phys. Chem. A*, 2012, **116**, 7943–7949.
- 20 C. W. West, J. N. Bull, A. S. Hudson, S. L. Cobb and J. R. R. Verlet, *J. Phys. Chem. B*, 2015, **119**, 3982–3987.
- 21 E. Carrascosa, J. N. Bull, M. S. Scholz, N. J. A. Coughlan, S. Olsen, U. Wille and E. J. Bieske, *J. Phys. Chem. Lett.*, 2018, **9**, 2647–2651.
- 22 N. J. A. Coughlan, M. H. Stockett, C. Kjær, E. K. Ashworth, P. C. B. Page, S. R. Meech, S. B. Nielsen, L. Blancafort, W. S. Hopkins and J. N. Bull, *J. Chem. Phys.*, 2021, **155**, 124304.
- 23 J. L. Woodhouse, A. Henley, R. Lewin, J. M. Ward, H. C. Hailes, A. V. Bochenkova and H. H. Fielding, *Phys. Chem. Chem. Phys.*, 2021, **23**, 19911–19922.
- 24 E. K. Ashworth, M. H. Stockett, C. Kjær, P. C. B. Page, S. R. Meech, S. B. Nielsen and J. N. Bull, *J. Phys. Chem. A*, 2022, **126**, 1158–1167.
- 25 E. K. Ashworth, J. Dezalay, C. R. M. Ryan, C. Ieritano, W. S. Hopkins, I. Chambrier, A. N. Cammidge, M. H. Stockett, J. A. Noble and J. N. Bull, *Phys. Chem. Chem. Phys.*, 2023, **25**, 20405–20413.
- 26 A. Svendsen, H. V. Kiefer, H. B. Pedersen, A. V. Bochenkova and L. H. Andersen, *J. Am. Chem. Soc.*, 2017, **139**, 8766–8771.
- 27 W. Zagorec-Marks, M. M. Foreman, J. R. R. Verlet and J. M. Weber, *J. Phys. Chem. Lett.*, 2019, **10**, 7817–7822.
- 28 L. H. Andersen, A. P. Rasmussen, H. B. Pedersen, O. B. Beletsan and A. V. Bochenkova, *J. Phys. Chem. Lett.*, 2023, **14**, 6395–6401.
- 29 T. T. Lindkvist, I. Djavani-Tabrizi, L. H. Andersen and S. B. Nielsen, *Phys. Rev. Lett.*, 2025, **134**, 093001.
- 30 N. H. List, C. M. Jones and T. J. Martínez, *Comm. Chem.*, 2024, **7**, 25.
- 31 S. Boyé, I. B. Nielsen, S. B. Nielsen, H. Krogh, A. Lapierre, H. B. Pedersen, S. U. Pedersen, U. V. Pedersen and L. H. Andersen, *J. Chem. Phys.*, 2003, **119**, 338–345.
- 32 J. Flotte de Pouzols, A. Subramani, E. K. Ashworth, J. N. Bull, H. Cederquist, J. Dezalay, N. H. List, P. Martini, J. E. N. Navarrete, H. T. Schmidt, H. Zettergren, B. Zhu and M. H. Stockett, *Phys. Rev. A*, 2025, **111**, 043112.
- 33 M. A. Parkes, A. Bennett and H. H. Fielding, *Mol. Phys.*, 2019, **117**, 3027–3035.
- 34 I. Alata, J. Bert, M. Broquier, C. Dedonder, G. Féraud, G. Grégoire, S. Soorkia, E. Marceca and C. Jouvét, *J. Phys. Chem. A*, 2013, **117**, 4420–4427.
- 35 J. A. Noble, E. Marceca, C. Dedonder, I. Carvin, E. Gloaguen and C. Jouvét, *Eur. Phys. J. D*, 2021, **75**, 1–13.
- 36 N. Esteves-López, C. Dedonder-Lardeux and C. Jouvét, *J. Chem. Phys.*, 2015, **143**, 074303.
- 37 G. A. Pino, R. A. Jara-Toro, J. P. Aranguren-Abrate, C. Dedonder-Lardeux and C. Jouvét, *Phys. Chem. Chem. Phys.*, 2019, **21**, 1797–1804.
- 38 J.-D. Chai and M. Head-Gordon, *Phys. Chem. Chem. Phys.*, 2008, **10**, 6615–6620.
- 39 T. H. Dunning, *J. Chem. Phys.*, 1989, **90**, 1007–1023.
- 40 M. J. Frisch, G. W. Trucks, H. B. Schlegel, G. E. Scuseria, M. A. Robb, J. R. Cheeseman, G. Scalmani, V. Barone, G. A. Petersson, H. Nakatsuji, X. Li, M. Caricato, A. V. Marenich, J. Bloino, B. G. Janesko, R. Gomperts, B. Mennucci, H. P. Hratchian, J. V. Ortiz, A. F. Izmaylov, J. L. Sonnenberg, D. Williams-Young, F. Ding, F. Lipparini, F. Egidi, J. Goings, B. Peng, A. Petrone, T. Henderson, D. Ranasinghe, V. G. Zakrzewski, J. Gao, N. Rega, G. Zheng, W. Liang, M. Hada, M. Ehara, K. Toyota, R. Fukuda, J. Hasegawa, M. Ishida, T. Nakajima, Y. Honda, O. Kitao, H. Nakai, T. Vreven, K. Throssell, J. A. Montgomery, Jr., J. E. Peralta, F. Ogliaro, M. J. Bearpark, J. J. Heyd, E. N. Brothers, K. N. Kudin, V. N. Staroverov, T. A. Keith, R. Kobayashi, J. Normand, K. Raghavachari, A. P. Rendell, J. C. Burant, S. S. Iyengar, J. Tomasi, M. Cossi, J. M. Millam, M. Klene, C. Adamo, R. Cammi, J. W. Ochterski, R. L. Martin, K. Morokuma, O. Farkas, J. B. Foresman and D. J. Fox, *Gaussian 16 Revision B.01*, 2016, Gaussian Inc. Wallingford



CT.

- 41 I. Sandler, J. Chen, M. Taylor, S. Sharma and J. Ho, *J. Phys. Chem. A*, 2021, **125**, 1553–1563.
- 42 A. K. Dutta, M. Saitow, B. Demoulin, F. Neese and R. Izsák, *J. Chem. Phys.*, 2019, **150**, 164123.
- 43 F. Neese, *WIREs Comput. Mol. Sci.*, 2011, **2**, 73–78.
- 44 F. Santoro, A. Lami, R. Improta, J. Bloino and V. Barone, *J. Chem. Phys.*, 2008, **128**, 224311.
- 45 P. Skurski, M. Gutowski and J. Simons, *Int. J. Quant. Chem.*, 2000, **80**, 1024–1038.
- 46 S. B. Nielsen, A. Lapierre, J. U. Andersen, U. V. Pedersen, S. Tomita and L. H. Andersen, *Phys. Rev. Lett.*, 2001, **87**, 228102.
- 47 E. Fermi and E. Teller, *Phys. Rev.*, 1947, **72**, 399–408.
- 48 J. Simons, *J. Phys. Chem. A*, 2008, **112**, 6401–6511.
- 49 Y.-R. Zhang, D.-F. Yuan and L.-S. Wang, *J. Phys. Chem. Lett.*, 2023, **14**, 7368–7381.
- 50 J. N. Bull, J. T. Buntine, M. S. Scholz, E. Carrascosa, L. Giacomozzi, M. H. Stockett and E. J. Bieske, *Faraday Discuss.*, 2019, **217**, 34–46.
- 51 J. N. Bull, C. S. Anstöter, M. H. Stockett, C. J. Clarke, J. A. Gibbard, E. J. Bieske and J. R. R. Verlet, *J. Phys. Chem. Lett.*, 2021, **12**, 11811–11816.
- 52 E. K. Ashworth, S. H. Ashworth and J. N. Bull, *Rev. Sci. Instrum.*, 2024, **95**, 075103.
- 53 E. K. Ashworth and J. N. Bull, *J. Chem. Phys.*, 2024, **161**, year.
- 54 J. A. Noble, E. Marceca, C. Dedonder and C. Jouvet, *Phys. Chem. Chem. Phys.*, 2020, **22**, 27290–27299.
- 55 J. N. Bull, C. W. West and J. R. R. Verlet, *Chem. Sci.*, 2015, **6**, 1578–1589.



All data that support the findings in this article are available from the corresponding author upon reasonable request.

[View Article Online](#)
DOI: 10.1039/D5CP02520F

